Contribution of the FAD Binding Site Residue Tyrosine 308 to the Stability of Pea Ferredoxin−NADP$^+$ Oxidoreductase†

Nora B. Calcaterra,‡ Guillermo A. Picó,§ Elena G. Orellano,‡ Jorgelina Ottado,‡ Néstor Carrillo,‡ and Eduardo A. Ceccarelli*,‡

Departments of Biological Sciences and Physical Chemistry, Facultad de Ciencias Bioquímicas y Farmacéuticas, Universidad Nacional de Rosario, Suipacha 531, (2000) Rosario, Argentina

Received May 2, 1995; Revised Manuscript Received July 17, 1995⊗

ABSTRACT: The contribution made by tyrosine 308 to the stability of pea ferredoxin−NADP$^+$ reductase was investigated using site-directed mutagenesis. The phenol side chain of the invariant carboxyl terminal tyrosine is stacked coplanar to the isoalloxazine moiety of the FAD cofactor. Fluorescence measurements indicate that this interaction plays a significant role in FAD fluorescent quenching by the reductase apoprotein. Replacement of the tyrosine by tryptophan or phenylalanine caused only a minor increase in the quantum yields of bound FAD, whereas nonaromatic substitutions to serine and glycine resulted in a large fluorescent rise. Results from NADP$^+$ titration experiments support a recent hypothesis [Karplus *et al.* (1991) *Science 251,* 60−66], suggesting that the phenol ring of Tyr 308 may fill the nicotinamide binding pocket in the absence of the nucleotide. The stability of the site-directed mutants, judged by thermal- and urea-induced denaturation studies, was lowered with respect to the wild-type enzyme. FNR variants harboring nonaromatic substitutions displayed more extensive destabilization. The decrease in thermodynamic stability correlated with the impairment of catalytic activities [Orellano *et al.* (1993) *J. Biol. Chem 268,* 19267−19273]. The results indicate that the presence of the electron-rich aromatic side chain adjacent to the isoalloxazine ring is essential for maximum stabilization of the FNR holoenzyme, resulting in a flavin conformation which optimizes electron flow between the prosthetic group and its redox partners.

Ferredoxin−NADP$^+$ oxidoreductases (FNR;[1] EC 1.18.1.2) represent an important class of flavoenzymes that utilize a noncovalently bound FAD cofactor as the only redox center. FNRs have been isolated from a wide variety of sources, in which they catalyze the reversible electron transfer between NADP(H) and electron carrier proteins like ferredoxin or flavodoxin (Shin & Arnon, 1965; Carrillo & Vallejos, 1987; Karplus & Bruns, 1994). In nonphototrophic bacteria and eucaryotes, the reaction is driven toward ferredoxin reduction, providing reducing power for a plethora of metabolic pathways. They include steroid hydroxylation in mammalian mitochondria (Hanukoglu & Gutfinger, 1989), nitrite reduction and glutamate synthesis in heterotrophic tissues of vascular plants (Ritchie *et al.,* 1994), and radical propagation and scavenging in *Escherichia coli* and other procaryotes (Krapp & Carrillo, 1995), as well as hydrogen and nitrogen fixation in anaerobes (Jungermann *et al.,* 1974). In chloroplasts and cyanobacteria, ferredoxin is reduced through a photochemical reaction at the level of photosystem I. FNR then mediates the electron transfer from the reduced iron−sulfur protein to NADP$^+$, providing the NADPH necessary for CO_2 fixation and other biosynthetic reactions (Carrillo & Vallejos, 1987, and references therein).

Plant FNRs are hydrophilic proteins of about 35 kDa, containing two different structural domains (Karplus & Bruns, 1994). The three-dimensional structure has been determined for the spinach enzyme at 0.17 nm resolution (Karplus *et al.,* 1991; Bruns & Karplus, 1995), contributing greatly to our understanding of the specific molecular interactions that exist between the flavin cofactor and the apoprotein. The prosthetic group is bound externally to an antiparallel β-barrel that makes up the core of the FAD binding domain at the amino terminal region of the flavoprotein (residues 20−162). The carboxyl terminal domain provides for binding of NADP$^+$, with the last 19 amino acids forming a distinct α-helix/β-strand region that folds back into the FAD site (Karplus *et al.,* 1991). The final tyrosine (corresponding to position 314 in spinach FNR and to position 308 in the pea enzyme) is one of two aromatic amino acids (the other being Tyr 95/89) that display the most extensive interaction with the isoalloxazine ring (Figure 1). These two residues are conserved in all plant-type FNRs thus far characterized (Karplus & Bruns, 1994, and references therein; see also Aoki & Ida, 1994; Ritchie *et al.,* 1994; Kitayama *et al.,* 1994). Moreover, aromatic amino acids have been identified in the flavin binding site of flavodoxin (Watt *et al.,* 1991) and of many other flavoproteins belonging to the FNR structural family (Andrews *et al.,* 1992), suggesting that they must play a significant role. The phenol ring of the terminal tyrosine in FNR is stacked coplanar to

† Supported by grants from the International Foundation for Science (IFS, Stockholm, Sweden) and Fundación Antorchas (Buenos Aires, Argentina). N.B.C., G.A.P., N.C., and E.A.C. are staff members and J.O. is a Fellow of the Consejo Nacional de Investigaciones Científicas y Técnicas (CONICET, Argentina).

* To whom all correspondence should be addressed. Fax: (54)(41)-300309, Phone: (54)(41)240010, Email: cecca@unrobi.edu.ar.

‡ Department of Biological Sciences.

§ Department of Physical Chemistry.

⊗ Abstract published in *Advance ACS Abstracts,* September 1, 1995.

[1] Abbreviations: FNR, ferredoxin−NADP$^+$ oxidoreductase (EC 1.18.1.2); GST, glutathione *S*-transferase (EC 2.5.1.18); DEAE, (diethylamino)ethyl; EDTA, ethylenediaminetetraacetic acid; SDS, sodium dodecyl sulfate.

0006-2960/95/0434-12842$09.00/0

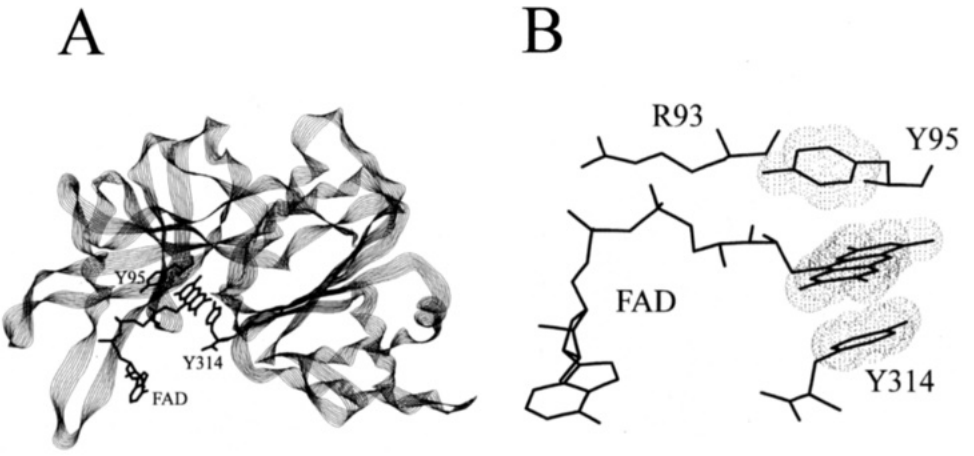

FIGURE 1: Computer graphics models showing the FAD environment in spinach ferredoxin−NADP$^+$ reductase. Representations are taken from X-ray crystal diffraction data (Karplus *et al.*, 1991). (A) Ribbon diagram of the FNR structure displaying the relative positions of the FAD cofactor and the flavin binding site residues Tyr 95 and Tyr 314. (B) Orientation of the two tyrosines flanking both faces of the FAD isoalloxazine ring. Dots represent the van der Waals surfaces of each aromatic system. The position of arginine 93, which binds the pyrophosphate group of FAD, is also included for comparison.

the *re* face of the isoalloxazine moiety and makes extensive π-orbital contact with it (Figure 1). As a consequence, the flavin group is partially shielded from solvent by this amino acid side chain (Karplus *et al.*, 1991).

Over the last years, site-directed mutagenesis has become the *sine qua non* for elucidating the role of amino acids in enzyme structure and catalysis. Using this approach in combination with kinetic and biophysical methods, Aliverti *et al.* (1991, 1993, 1994) have extensively characterized the functional lysyl and cysteinyl residues of spinach FNR. The role of the carboxyl terminal tyrosine in the pea flavoprotein was also investigated through the introduction of several amino acid substitutions at position 308. Of these, the FNR forms carrying aromatic mutations were the most active, displaying 50% residual activity. Changes to nonaromatic side chains caused a major impairment in the catalytic efficiency of the resulting enzymes (Orellano *et al.*, 1993). K_M values for various substrates were largely unaffected by the substitutions. Even the complete removal of the terminal tyrosine had no remarkable effect on the affinity of the enzyme for NADPH or ferredoxin, while causing a 850-fold decrease in k_{cat} (Orellano *et al.*, 1993). The results indicated that (i) aromaticity was the most important factor to the function of the tyrosine in FNR and (ii) all tyrosine substitutions were shown to introduce barriers only to catalysis, without affecting the interaction with substrates.

This effect on k_{cat} might be related to a direct involvement of the tyrosine in catalysis, or to a structural role in FNR folding, FAD attachment, or both. The location of the residue at the surface of the flavoprotein makes it unlikely that its replacement may introduce structural perturbations to the protein backbone *per se*, unless FAD binding is involved. We have previously advanced the hypothesis that the presence and proper orientation of the tyrosine might be necessary for a correct docking of the flavin molecule in its binding pocket during holoenzyme assembly. In the present study, we use FAD fluorescence measurements, thermal unfolding, and transverse urea gradient gel electrophoresis to demonstrate that Tyr 308 plays a key role in FNR holoprotein stability.

MATERIALS AND METHODS

Expression and Purification of Ferredoxin−NADP$^+$ Reductase Variants. DNA sequences encoding the mature region of pea FNR (Newman & Gray, 1988) were ligated in-frame to the 3′ end of the glutathione *S*-transferase gene in plasmid pGEX-3X (Smith & Johnson, 1988). A full description of the procedures employed for cloning, mutagenesis, and overexpression of the pea FNR mutants Y308W, Y308F, Y308S, and Y308G has been reported elsewhere (Ceccarelli *et al.*, 1991; Serra *et al.*, 1993; Orellano *et al.*, 1993). The various flavoproteins were purified from *E. coli* JM109 lysates essentially as described before (Serra *et al.*, 1993), except that the protease Xa digest was directly applied onto a DEAE-cellulose column equilibrated in 50 mM Tris-HCl, pH 7.6. The column was extensively washed with the same buffer, and bound FNR was eluted using a linear gradient of NaCl (0−400 mM) in 50 mM Tris-HCl, pH 7.6. The fraction eluting at about 250−300 mM NaCl contained homogeneous FNR protein. Samples were extensively dialyzed against 4 mM sodium phosphate, pH 7.2, and concentrated by freeze-drying. Purification was followed by measuring total protein (Sedmak & Grossberg, 1977) and ferricyanide reductase (diaphorase) activity (Serra *et al.*, 1993). The purity of each preparation was confirmed by SDS−polyacrylamide gel electrophoresis (Laemmli, 1970).

Preparation of FNR apoproteins and reconstitution with free FAD were carried out essentially as described by Zanetti *et al.* (1982).

Fluorescence Measurements. The concentrations of the different FNR variants were determined by measuring the flavin released in 5% (w/v) trichloroacetic acid (Swenson & Krey, 1994), using high performance liquid chromatography and fluorescence detection (Carrillo, 1985). All determinations were carried out in triplicate. Pure FAD, subjected to the same treatment, was used as a control. Fluorescence excitation and emission spectra were recorded at 25 °C in 20 mM sodium phosphate, pH 7.2, using a Jasco FP-770 spectrofluorometer.

To obtain the FAD emission spectrum of FNR, the excitation wavelength was fixed at 456 nm. Relative quantum yields were calculated according to Pesce *et al.* (1991). Energy transfer was determined by following the increase in FAD fluorescence at 526 nm after excitation of the FNR samples at 295 nm.

Thermal Unfolding Transitions. Protein stock solutions were diluted to a final concentration of 0.3 mg/mL in 20 mM sodium phosphate, pH 7.2. Intrinsic tryptophan fluo-

rescence was monitored on the Jasco FP-770, with a 1-cm-path water-jacketed cuvette, by exciting at 280 nm and recording the emission at 345 nm. The temperature of the sample was increased at a uniform rate of 0.7 °C/min and the fluorescence signal averaged over 30-s intervals. The thermal unfolding transitions were analyzed assuming a two-state approximation in which only the native and unfolded states are significantly populated and the quantum yields of the two states are different. The fluorescence (F) *vs* temperature (T) curves were fitted by nonlinear regression to obtain values for the temperature at the midpoint of unfolding (T_m), using the following equation (Pace *et al.*, 1990):

$$\alpha = \frac{F_N + m_N T - F}{F_N + m_N T - F_U + m_U T}$$

in which α represents the fraction of protein in the unfolded conformation, while F_N and F_U are the fluorescence of the native and unfolded states, respectively, at some reference temperature (0 °C). The slopes of the pre- and post-transition regions (m_N and m_U, respectively) describe the linear dependence of the fluorescence of the native and denatured proteins with temperature (Pace *et al.*, 1989, 1990).

Urea Gradient Gel Electrophoresis. Urea gradient gels were prepared according to Creighton (1986) with some modifications. Briefly, 50 mM Tris−acetate, pH 8.0, was used to prepare 1-mm-thick polyacrylamide gels containing a horizontal linear gradient of 0−8 M urea and a compensatory inverse gradient of 7.0−5.5% (w/v) acrylamide. Gradient uniformity among the different gels was accomplished by the use of a casting box that allows the simultaneous preparation of several gels.

Electrophoresis of the different FNR variants was performed using either native or urea-unfolded reductase. In order to reduce any oxidized cysteine or methionine residues, the FNR proteins were first incubated (20 min at 30 °C) in 20 mM sodium phosphate, pH 7.2, 2 mM EDTA, and 10 mM dithiothreitol. FNR unfolding was carried out by a subsequent 40-min incubation at 25 °C in 8 M urea. The native and unfolded samples of each FNR variant were then diluted to 0.2 mg/mL in Tris−acetate buffer, pH 8.0, 10% (v/v) glycerol, and 20 μg/mL bromophenol blue and finally applied (100 μL) to identical gels that had been preelectrophoresed for 20 min. The temperature of the gel was kept at 12 °C with the aid of a Midget LKB 2050 refrigeration unit and a flexible thermocouple microprobe attached to the glass plate.

After completion of electrophoresis, polyacrylamide gels were stained for FNR activity. A 3 MM Whatman paper was soaked in a medium containing 50 mM Tris-HCl, pH 8.0, 0.8 mM $NADP^+$, 0.5 mg/mL nitroblue tetrazolium, 3 mM glucose 6-phosphate, and 1 unit/mL glucose-6-phosphate dehydrogenase. The gels were placed onto the wet paper starting from the low urea concentration side and avoiding the formation of air bubbles. The setup was incubated for 30 min at 37 °C in a humid chamber. FNR diaphorase activity was visualized by the formation of a purple formazan precipitate on a yellowish background. Following activity development and recording, the same gels were either silver stained (Blum *et al.*, 1987) or subjected to electroblotting and immunoreaction with rabbit anti-FNR antisera (Towbin *et al.*, 1979).

Table 1: FAD Fluorescent Properties of Wild-Type and Mutant Ferredoxin−$NADP^+$ Reductases in the Oxidized Form

FNR variant	relative quantum yields[a]		relative energy transfer[b]
		+0.1 mM $NADP^+$	
wild-type	0.75 ± 0.21	1.95 ± 0.28	1
Y308W	1.08 ± 0.20	1.98 ± 0.24	1.89 ± 0.16
Y308F	1.03 ± 0.14	1.54 ± 0.19	1.04 ± 0.17
Y308S	5.40 ± 0.34	5.07 ± 0.44	0.98 ● 0.12
Y308G	7.11 ± 0.35	6.88 ± 0.40	1.01 ± 0.08

[a] Relative quantum yields of the various proteins are expressed as the percentage of the emissions at 526 nm relative to that of free FAD at the same concentration. In all cases, the samples were excited at 456 nm. [b] Energy transfer was determined by measuring FAD fluorescence emission at 526 nm upon excitation of the FNR proteins at 295 nm. Values are expressed relative to the emission of the wild-type flavoprotein measured under identical conditions.

Rate constants for unfolding at the transition midpoints were estimated from the continuity or discontinuity of the gel bands, which depends upon the rate of unfolding relative to the time of electrophoresis. The observed distributions of stained protein at the midpoint were compared to those predicted for different arbitrary values of the unfolding rate constants (Creighton, 1979; Goldenberg & Creighton, 1984).

RESULTS

FAD Fluorescence of Ferredoxin−$NADP^+$ Reductase Mutants. The environment of bound FAD in various 308-position mutants was probed by measuring the intrinsic flavin fluorescence of the native proteins. The fluorescent emission maximum was 526 nm for all FNR variants (not shown), and the corresponding quantum yields are summarized in Table 1. The fluorescence of bound FAD is known to be largely quenched in the native oxidized form of wild-type FNR (Forti, 1966; Shin, 1973). Accordingly, we observed that the emission of the pea flavoenzyme at 526 nm was only 0.75% of that of free FAD (Table 1), consistent with the value of 0.6% reported by Shin (1973). Mutants containing an aromatic residue at position 308 (Y308W and Y308F) displayed only small increases of the relative quantum yields, whereas removal of the aromatic side chain in the Y308G and Y308S variants caused a large fluorescent rise (Table 1). These results indicate that the interaction between Tyr 308 and the isoalloxazine ring in the wild-type flavoprotein (Karplus *et al.*, 1991; Figure 1) accounts for a significant fraction of the total FAD fluorescence quenching in native FNR. The behavior of the tryptophan and phenylalanine substitutions suggests that aromaticity is the key factor involved in quenching and that the aromatic residues introduced in the mutants adopt a conformation similar to that of Tyr 308 in the wild-type enzyme (Table 1). Indeed, significant energy transfer between the indole side chain of Trp 308 and the isoalloxazine ring was observed in the Y308W mutant (Table 1), indicating that the two fluorophores are still close to each other in this FNR variant.

Shin (1973) has reported that spinach FNR undergoes FAD fluorescence enhancement upon complex formation with $NADP^+$. Following addition of the nucleotide, significant increases in quantum yield were actually observed for the wild-type recombinant FNR, the Y308W variant, and to a lesser extent, the phenylalanine mutant (Table 1). In all cases, the amplitude of the fluorescent rise was titrated by $NADP^+$ with an apparent K_D of 7−17 μM and an $NADP^+$/

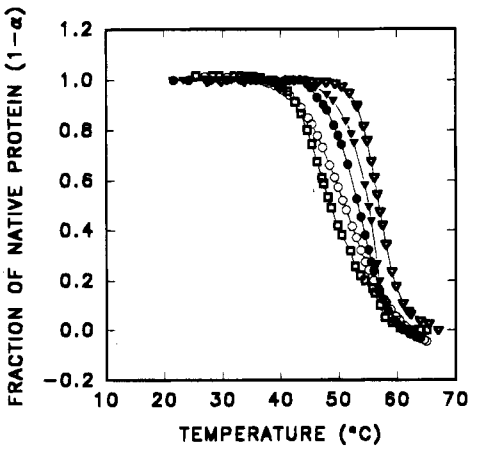

FIGURE 2: Thermal unfolding transitions of ferredoxin−NADP$^+$ reductase variants. Denaturation profiles of wild-type FNR (▽), and mutants Y308W (●), Y308F (▼), Y308S (○), and Y308G (□) were monitored by the decrease in tryptophan fluorescence upon heating at a rate of 0.7 °C/min. Experimental details and calculation procedures are given under Materials and Methods.

FNR stoichiometry of 1.07−1.22 (not shown). Addition of NADP$^+$ to FNR mutants containing nonaromatic replacements at the carboxyl terminal position resulted in FAD fluorescence quenching, rather than enhancement (Table 1), even when nucleotide binding must have occurred under the conditions of the assay (Orellano *et al.*, 1993). These results suggest that the NADP$^+$-driven fluorescent rise is caused by a breakdown of the stacked interaction between the flavin and aromatic side chains at position 308 of the apoprotein.

Analysis of Thermal Denaturation Curves. The thermal stabilities of wild-type and mutant FNRs were measured by monitoring the decrease in the intrinsic fluorescence of tryptophan as a function of temperature. FNR unfolding followed a typical sigmoidal behavior (Figure 2). The denatured enzyme could not be refolded by cooling the sample, presumably due to FAD release during denaturation (not shown).

Thermal denaturation curves were analyzed on the basis of the two-state model (Pace *et al.*, 1989), and the temperatures at the midpoint of the unfolding transitions (T_m) are given in Table 2 for the five FNR variants. Table 2 also shows the corresponding ΔS_m values (entropy change at T_m), calculated from the slopes of ΔG *vs* T at the midpoint temperatures (Pace *et al.*, 1989). All replacements led to less stable enzymes compared to the wild-type, with the nonaromatic mutants Y308G and Y308S showing the lowest stability (Table 2). Therefore, the structural consequences of single substitutions at the carboxyl terminal position of FNR followed a similar trend as that observed for enzyme activity (Orellano *et al.*, 1993).

Substitutions at the 308 position caused only minor changes in the affinity of the various apoenzymes for FAD (Table 2), suggesting that the decrease in thermodynamic stability was not due to a facilitated release of the prosthetic group in the more destabilized FNR forms.

Urea-Induced Unfolding Transitions of Ferredoxin−NADP$^+$ Reductase Variants. To further characterize the effect of Tyr 308 substitutions on FNR stability, wild-type and four mutant enzymes were subjected to transverse urea gradient gel electrophoresis. In this method, unfolding is detected by the reduced mobility of the denatured form of the protein, and the resulting electrophoretic pattern provides semiquantitative information about the stability of the native enzyme and the rate of the unfolding transition (Creighton, 1979; Goldenberg & Creighton, 1984). The presence of the different FNR conformations was detected in the gels using either silver staining, immunoblotting, or *in situ* activity measurements. Typical results obtained with the three methods are compared for the Y308W mutant in Figure 3. Silver or antibody detection revealed identical transitions (Figure 3a,b), with immunoreaction showing the highest sensitivity levels. The detection limits of functional FNR species by activity staining were even lower than those of immunoblotting (Figure 3c). The denatured form of the Y308W mutant did not refold when electrophoresed in urea gradient gels (Figure 3d). Similar results were obtained with the wild-type and the three other mutant FNRs under all electrophoretic conditions tested (not shown).

When the five FNR variants were applied to urea gradient gels and electrophoresed for 35 min at 250 V, the different proteins displayed discontinuous unfolding transitions with a wide range of midpoint urea concentrations (Figure 4A). In many samples, the immunoreaction revealed the existence of at least two native FNR forms with different electrophoretic mobilities (Figures 3b and 4A). They presumably arise from the reported proteolytic lability of the FNR amino terminus (reviewed in Carrillo & Vallejos, 1987). In all cases, the various forms migrated as a single band above the transition midpoint (Figure 3b).

During high-voltage electrophoresis, the wild-type flavoprotein underwent two separate unfolding transitions upon increasing the urea concentration (Figure 4A). This effect could not be observed during thermal denaturation (Figure 2), or when electrophoresis was carried out at lower voltage (see below). Replacement of the tyrosine by tryptophan, phenylalanine, serine, and glycine resulted in single transitions progressively displaced toward lower urea concentrations (Figure 4A).

Figure 4B shows the results obtained when the urea gels were stained for FNR activity. Wild-type FNR was inactivated above 5 M urea, which agrees remarkably well with results obtained previously in solution experiments (Zanetti & Forti, 1966). Inactivation of the four FNR mutants occurred at lower urea concentrations, showing a good correlation with the unfolding profiles of Figure 4A. Functional forms of the reductase were strictly associated to the various native species, as demonstrated by the constant mobility of the activity band(s) across the gel (Figure 4B). The partially folded FNR form observed during denaturation of wild-type FNR was devoid of enzymatic activity (Figure 4), indicating that catalysis was impaired at the initial stages of denaturation.

Conditions used to generate the FNR profiles of Figure 4A led to discontinuous transitions for the wild-type and the four 308-position mutants, indicating that unfolding rates at the transition midpoints were slow on the time scale of electrophoresis. Blurred bands were generated when the five different flavoproteins were electrophoresed for longer times (300 min) at lower voltages (10 V), suggesting that the transition rates at the midpoints were in the time range of electrophoresis. Typical results are shown in Figure 5 for the wild-type, the Y308W, and the Y308F flavoproteins. An estimation of the rate constants for unfolding at the transition midpoints (Creighton, 1979; Goldenberg & Creighton, 1984) yielded values in the range of $(5-25) \times 10^{-3}$ min^{-1}. No significant differences were observed among the various FNR variants (not shown). The two separate transitions of the

Table 2: Thermodynamic Parameters Characterizing the Thermal- and Urea-Induced Unfolding of Wild-Type Ferredoxin−NADP$^+$ Reductase and Four Mutants at Position 308

FNR protein	T_m[a] (°C)	ΔS_m[b] [kcal/(mol·deg)]	$\Delta\Delta G_u$[c] (kcal/mol)	C_m[d] (M)	m[e] [kcal/(mol·M)]	$\Delta\Delta G_u$[f] (kcal/mol)	$\Delta\Delta G_{(cat)}$[g] (kcal/mol)	K_D (FAD)[h] (nM)
wild-type	57.0 ± 0.2	0.29 ± 0.03		4.7 ± 0.3	1.30 ± 0.15			4.7 ± 1.8
Y308W	53.9 ± 0.3	0.22 ± 0.01	0.8	4.0 ± 0.2	1.25 ± 0.12	0.9	0.5	3.9 ± 1.7
Y308F	55.4 ± 0.1	0.19 ± 0.01	0.5	3.3 ± 0.2	1.30 ± 0.14	1.8	0.4	nd[i]
Y308S	51.0 ± 0.3	0.19 ± 0.01	1.8	2.7 ± 0.2	1.40 ± 0.18	2.6	1.9	5.9 ± 1.9
Y308G	48.5 ± 0.3	0.25 ± 0.02	2.5	2.2 ± 0.3	1.25 ± 0.15	3.2	3.3	5.6 ± 1.4

[a] Midpoint of thermal unfolding curves (Figure 2). [b] ΔS_m values were calculated from the slope of ΔG *vs* T at T_m, essentially as described by Pace *et al.* (1989). [c] $\Delta\Delta G_u$ represents the change in conformational stability caused by the different mutations, as determined from thermal denaturation profiles. $\Delta\Delta G_u = \Delta(T_m) \times \Delta S_m$(wild-type). [d] Midpoint of the urea unfolding curves. Taken from experiments such as those depicted in Figure 5B. [e] Slope of ΔG *vs* urea concentration at C_m. Both C_m and m were determined in gels that were electrophoresed for 300 min at 10 V in order to obtain blurred transitions. Under these conditions, wild-type FNR displayed a single unfolding transition (Figure 5B). [f] $\Delta\Delta G_u$ represents the change in thermodynamic stability of the proteins introduced by the mutations, as determined from urea unfolding curves. $\Delta\Delta G_u = \Delta(C_m) \times m$(wild-type) (Pace *et al.*, 1989). [g] Mutation-induced increases in the free energy of activation for FNR activities. Averaged from data reported by Orellano *et al.* (1993). [h] K_D values were determined by FAD titration of the corresponding apoproteins (Zanetti *et al.*, 1982). A 1:1 stoichiometry between flavin and protein was obtained in all cases. [i] nd, not determined.

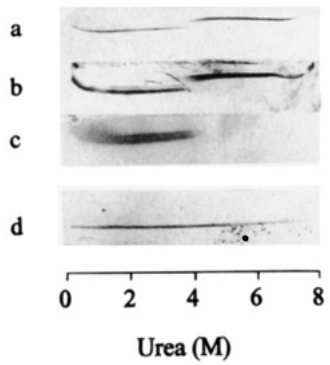

FIGURE 3: Urea gradient gel electrophoresis patterns of the Y308W mutant version of ferredoxin−NADP$^+$ reductase. Experimental conditions are given in the text. Native (a−c) or unfolded (d) Y308W FNR was electrophoresed for 35 min at 250 V, and the gels were subjected to silver staining (a and d), electroblotting and immunoreaction (b), or activity staining (c).

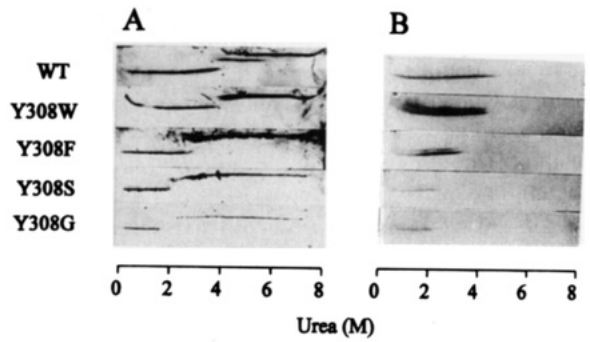

FIGURE 4: Urea-induced unfolding transitions of wild-type and mutant ferredoxin−NADP$^+$ reductases. The native proteins were subjected to transverse urea gradient gel electrophoresis (35 min at 250 V). Proteins were visualized by blotting and immunodetection (A) or diaphorase activity staining (B).

wild-type FNR occurring at 250 V could not be resolved kinetically under the lower voltage conditions, leading to a monophasic profile with an intermediate C_m of 4.7 ± 0.4 M (Figure 5B).

The urea concentrations at the transition midpoints (C_m) were used to calculate the differences in stability relative to the wild-type ($\Delta\Delta G_u$), introduced by the mutations (Pace *et al.*, 1989). The corresponding values are summarized in Table 2. In agreement with the thermal denaturation profiles, substitutions of Tyr 308 resulted in C_m values below that of the wild-type flavoprotein, with nonaromatic replacements leading to more extensively destabilized forms (Table 2).

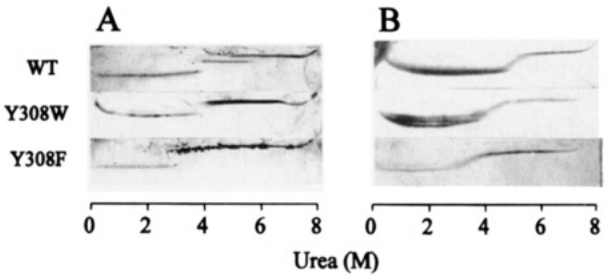

FIGURE 5: Estimation of the unfolding rate constants for the wild-type, Y308W, and Y308F variants of ferredoxin−NADP$^+$ reductase. The native FNR proteins were electrophoresed at 250 V for 35 min (A) or at 10 V for 300 min (B), transferred to nitrocellulose membranes, and detected by immunoreaction.

DISCUSSION

A variety of amino acids were replaced for the invariant tyrosyl residue at the carboxyl terminus of pea ferredoxin−NADP$^+$ reductase, and the effects of these changes on the FAD fluorescence and the stability of the flavoprotein were investigated. Results obtained in the course of this study provide rationales for a range of FNR properties that had been known for years. The extensive quenching of the intrinsic FAD fluorescence in native FNR was first observed by Forti (1966) and was assumed to indicate that the flavin cofactor was hidden by amino acids within the protein backbone (reviewed in Carrillo & Vallejos, 1987). Later, X-ray diffraction data showed that the flavin group is actually bound externally to the FAD binding domain, which covers only the back (*si* face) of the isoalloxazine ring (Karplus *et al.*, 1991; Bruns & Karplus, 1995). Shielding of the *re* face from solvent is partially accomplished by stacking with the phenol side chain of Tyr 308 and is limited to the pyrimidine and pyrazine rings (Zanetti *et al.*, 1983; Karplus *et al.*, 1991). Karplus and co-workers (1991) have proposed that this aromatic interaction could explain the effective quenching of flavin fluorescence in the native flavoprotein. Our results are consistent with this hypothesis. Replacement of Tyr 308 by tryptophan or phenylalanine had little effect on the relative quantum yield, but removal of the bulky aromatic side chain in the Y308S and Y308G mutants resulted in a dramatic enhancement of FAD fluorescence (Table 1). This effect is observed even when collisional quenching should be expected to increase as a consequence of higher flavin exposure to solvent in the nonaromatic mutants. We therefore propose that the phenol side chain of Tyr 308 behaves as a static quencher of the flavin moiety, presumably by enhancing

nonradiative deactivation of the first excited singlet (Pesce *et al.*, 1991).

Our results also support the hypothesis that, in the FNR−NADP$^+$ complex, the side chain of Tyr 308 is displaced from its original position in the native flavoprotein by the entering nicotinamide (Karplus *et al.*, 1991). According to this model, breakdown of the phenol−flavin quenching complex upon nucleotide binding should cause an enhancement of the intrinsic FAD fluorescence of FNR. Early observations confirm the prediction for the wild-type flavoprotein (Shin, 1973), and results presented in Table 1 extend it to the Y308W and the Y308F variants. As expected, NADP$^+$ binding failed to enhance the FAD fluorescence of the nonaromatic mutants Y308S and Y308G (Table 1). On the other hand, substitutions of Tyr 308 had no remarkable effect on the K_M for NADP$^+$ (Orellano *et al.*, 1993), suggesting that movement of the phenol side chain does not play any significant role in nucleotide binding. It is possible that docking of NADP$^+$ to FNR is primarily determined by the phospho-AMP portion of the nucleotide. Indeed, X-ray diffraction data and biochemical experiments with site-directed mutants revealed the existence of a number of interactions between the protein and the phospho-AMP moiety (Karplus *et al.*, 1991; Aliverti *et al.*, 1991; Bruns & Karplus, 1995).

Mutations at position 308 are not expected to introduce gross conformational changes into FNR. The modified residue is located at the carboxyl terminus and on the surface of the protein, so that rearrangements in the mutant FNRs should be limited to those required to accommodate the new side chain in the immediate environment of the FAD group. Modeling analyses using the crystallographic data of the wild-type flavoprotein (Karplus *et. al.*, 1991) indicate that the *re* face of the isoalloxazine ring is large enough to accommodate even the bulky aromatic side chain of tryptophan. Moreover, Trp 308 in the Y308W variant is sufficiently close to the flavin group to allow significant energy transfer between the indole and the isoalloxazine rings (Table 1).

Substitutions of Tyr 308 were shown to destabilize the native conformation of FNR mutants with respect to the wild-type, as revealed by thermal- and urea-induced denaturation studies (Figure 2−5). The approaches used to estimate the differences in stability, $\Delta\Delta G_u$, from the two types of data are described in Table 2. The absolute conformational stabilities of the various proteins under ambient conditions (*i.e.*, in water at 25 °C) can be described by the free energy change of the unfolding reaction. Estimates from thermal or urea denaturation curves are termed ΔG(25 °C) and $\Delta G(H_2O)$, respectively (Pace, 1990). Calculation of these values is however hazardous because errors in the experimental measurements are magnified by the extrapolations required to obtain the free energy changes under the two different sets of conditions (Pace *et al.*, 1989). On the contrary, $\Delta\Delta G_u$ estimations are less prone to error, since they are based on differences in T_m and C_m, which can be determined accurately and referred to the ΔS_m and m values of the wild-type enzyme (Pace *et al.*, 1989). The $\Delta\Delta G_u$ values obtained from both types of denaturation procedures showed a similar profile, although significant differences did exist (Table 2). This is not unexpected since the calculations apply to two different sets of experimental conditions (namely, those existing near the midpoints of the unfolding curves), and the urea and thermal denaturations do not necessarily proceed along similar pathways. FNR unfolding by either method led to irreversibly denatured forms, presumably resulting from holoenzyme dissociation (Zanetti & Forti, 1966). The shape of the thermal denaturation curves and the calculated ΔS_m values (Table 2) suggest that the destabilization introduced by the various mutations was not entirely enthalpic.

Data summarized in Table 2 also indicate that the presence of a nonaromatic residue at position 308 is more detrimental for FNR stability. No correlation was observed between the transition midpoints and the unfolding rates estimated in urea gradient gels (Figure 5). The decrease in thermodynamic stability introduced by destabilizing substitutions like Y308S (2.5 kcal/mol) or Y308G (3.2 kcal/mol) was not expressed kinetically as increased unfolding rates relative to the wild-type. Therefore, it is apparent that at least part of the destabilization introduced by amino acid replacements at position 308 occurs between the transition state and the unfolded state and that it should have a significant effect upon folding rates (Klemm *et al.*, 1991, and references therein). Indeed, we observed that major alterations at this position resulted in lower accumulation, lack of FAD binding, and/or precipitation of the recombinant reductase in *E. coli* cells (see Figure 4 in Orellano *et al.*, 1993). On the other hand, results obtained upon FNR reconstitution *in vitro* suggest that these effects are not determined by changes in FAD affinity (Table 2), but more likely by alterations in the stability of the holoprotein structure. *In toto*, the previous considerations strongly suggest that holoenzyme biogenesis (and stability) is quite sensitive to the presence of an aromatic side chain (preferably tyrosine) at the flavin binding site of FNR proteins.

Since the enzymatic activities of all five FNR species have been determined previously (Orellano *et al.*, 1993), the stability data for the mutant proteins can be compared to those of the wild-type enzyme in the context of catalytic differences. Mutations at the carboxyl terminal position are known to introduce barriers only to catalysis, without affecting the affinity of the flavoprotein for natural or artificial substrates (Orellano *et. al.*, 1993). The energetic magnitudes of those barriers are in reasonable agreement with the changes in $\Delta\Delta G_u$ calculated from unfolding experiments (Table 2), indicating that the increases in the free energy of activation introduced by replacement of Tyr 308 are largely accounted for by reductions in the thermodynamic stability of the corresponding holoproteins.

The exact nature of this effect remains to be established. The coplanar geometry of the isoalloxazine and phenol rings in FNR is truly remarkable. It has been observed to occur at the opposite face of the flavin in flavodoxins (Watt *et al.*, 1991; Swenson & Krey, 1994) and inferred from sequence data in NADPH−cytochrome P450 reductase (Shen *et al.*, 1989). Similar interactions have been invoked in a few other cases, including the formation of a coplanar complex between phenol and nicotinamide during NAD$^+$ binding to diphtheria toxin (Blanke *et al.*, 1994). Contrary to common belief, however, stacked geometries that maximize π-orbital overlap are energetically unfavorable, and this type of arrangement can only be established when the aromatic moieties have complementary charges or polarizations that lead to attractive electrostatic interactions (Hunter & Sanders, 1990; Hunter *et al.*, 1991). Indeed, estimations of the charge distribution in the stacked phenol−flavin complex of FNR support the

prevalence of electrostatic stabilization (A. Vila, unpublished).

Although elucidation of the way(s) in which this electrostatic interaction may determine the stability and/or the catalytic efficiency of the flavoprotein will require further experimental work, some hypotheses can be advanced based on the available data. We have previously suggested that the presence of a tyrosine (or other aromatic residue) at the carboxyl terminal position of FNR is required for proper accommodation of the FAD group in its binding cleft during holoenzyme assembly *in vivo* (Orellano *et al.*, 1993). An alternative possibility emerges from the results obtained by Swenson and Krey (1994) with flavodoxin. These authors observed that mutagenesis of Tyr 98 (which is stacked to the isoalloxazine ring in that protein) induced changes in the redox potential of the bound FMN cofactor. Solution studies suggested that tyrosine might assist in the thermodynamic stabilization of the neutral flavin semiquinone through preferential complex formation relative to the other oxidation states (Swenson & Krey, 1994). The participation of the FNR apoprotein in stabilizing the flavin semiquinone radical has been recognized for years (Huang *et al.*, 1969), and the involvement of Tyr 308 in this process is currently under investigation, on both theoretical and experimental grounds.

Although the tryptophan and phenylalanine mutants were designed to be conservative substitutions for Tyr 308, the two aromatic amino acids were not able to fully replace the functions of the wild-type residue. The corresponding FNR variants showed decreased activity (Orellano *et al.*, 1993) and stability (this work), suggesting that although aromaticity is the key factor to the function of Tyr 308 in FNR, the hydroxyl group of the phenol side chain also plays a significant role in establishing a functional conformation. This effect might explain why aromatic substitutions of the carboxyl terminal tyrosine are not observed in the dozen of FNR sequences already available. It is likely that the results presented here, together with structural and functional studies on other FNR mutants with altered FAD binding sites, will lead to a better understanding as to how these proteins can so dramatically modulate the properties of the versatile flavin coenzyme.

ACKNOWLEDGMENT

The authors wish to thank Dr. J. C. Gray (University of Cambridge, U.K.) for the generous gift of the original FNR cDNA clone and Dr. A. Vila (Biophysics Section, University of Rosario, Argentina) for critical reading of the manuscript and many helpful discussions.

REFERENCES

Aliverti, A., Lübberstedt, T., Zanetti, G., Herrmann, R. G., & Curti, B. (1991) *J. Biol. Chem. 266*, 17760−17763.
Aliverti, A., Piubelli, L., Zanetti, G., Lübberstedt, T., Herrmann, R. G., & Curti, B. (1993) *Biochemistry 32*, 6374−6380.
Aliverti, A., Corrado, M. E., & Zanetti, G. (1994) *FEBS Lett. 343*, 247−250.
Andrews, S. C., Shipley, D., Keen, J. N., Findlay, J. B., Harrison, P. M., & Guest, J. R. (1992) *FEBS Lett. 302*, 247−252.
Aoki, H., & Ida, S. (1994) *Biochim. Biophys. Acta 1183*, 553−556.
Blanke, S. R., Huang, K., & Collier, R. J. (1994) *Biochemistry 33*, 15494−15500.
Blum, H., Beier, H., & Gross, H. (1987) *Electrophoresis 8*, 93−99.
Bruns, C. M., & Karplus, P. A. (1995) *J. Mol. Biol.* 247, 125−145.
Carrillo, N. (1985) *Eur. J. Biochem. 150*, 469−474.
Carrillo, N., & Vallejos, R. H. (1987) in *The Light Reactions. Topics in Photosynthesis* (Barber, J., Ed.) Vol. 8, pp 527−560, Elsevier, Amsterdam, New York, and Oxford.
Ceccarelli, E. A., Viale, A. M., Krapp, A. R., & Carrillo, N. (1991) *J. Biol. Chem. 266*, 14283−14287.
Creighton, T. E. (1979) *J. Mol. Biol. 129*, 235−264.
Creighton, T. E. (1986) *Methods Enzymol. 131*, 156−172.
Forti, G. (1966) *Brookhaven Symp. Biol. 19*, 195−201.
Goldenberg, D. P., & Creighton, T. E. (1984) *Anal. Biochem. 138*, 1−18.
Hanukoglu, I., & Gutfinger, T. (1989) *Eur. J. Biochem. 180*, 479−484.
Huang, K., Tu, S. I., & Wang, J. H. (1969) *Biochem. Biophys. Res. Commun. 34*, 48−52.
Hunter, C. A., & Sanders, J. K. M. (1990) *J. Am. Chem. Soc. 112*, 5525−5534.
Hunter, C. A., Singh, J., & Thornton, J. M. (1991) *J. Mol. Biol. 218*, 837−846.
Jungermann, K., Kirchniawy, H., Katz, N., & Thauer, R. K. (1974) *FEMS Microbiol. Lett. 43*, 203−206.
Karplus, P. A., & Bruns, C. (1994) *J. Bioenerg. Biomembr. 26*, 89−99.
Karplus, P. A., Daniels, M. J., & Herriott, J. R. (1991) *Science 251*, 60−66.
Kitayama, M., Kitayama, K., & Togasaki, R. K. (1994) *Plant Physiol. 106*, 1715−1716.
Klemm, J. D., Wozniak, J. A., Alber, T., & Goldenberg, D. P. (1991) *Biochemistry 30*, 589−594.
Krapp, A. R., & Carrillo, N. (1995) *Arch. Biochem. Biophys. 317*, 215−221.
Laemmli, U. K. (1970) *Nature 227*, 680−685.
Newman, B. J., & Gray, J. C. (1988) *Plant Mol. Biol. 10*, 511−520.
Orellano, E. G., Calcaterra, N. B., Carrillo, N., & Ceccarelli, E. A. (1993) *J. Biol. Chem. 268*, 19267−19273.
Pace, C. N. (1990) *Trends Biotechnol.* 8, 93−98.
Pace, C. N., Shirley, A., & Thomson, J. A. (1989) in *Protein Structure. A Practical Approach* (Creighton, T. E., Ed.) pp 311−330, IRL Press, Oxford, New York, and Tokyo.
Pace, C. N., Laurents, D., & Thomson, J. A. (1990) *Biochemistry 29*, 2564−2571.
Pesce, A., Rosen, C. G., & Pasby, T. (1991) *Fluorescence Spectroscopy*, Marcel Dekker, New York.
Ritchie, S. W., Redinbaugh, M. G., Shiraishi, N., Vrba, J. M., & Campbell, W. H. (1994) *Plant Mol. Biol. 26*, 679−690.
Sedmak, J., & Grossberg, S. (1977) *Anal. Biochem. 79*, 544−552.
Serra, E. C., Carrillo, N., Krapp, A. R., & Ceccarelli, E. A. (1993) *Protein Expression Purif. 4*, 539−546.
Shen, A. L., Porter, T. D., Wilson, T. E., & Kasper, C. B. (1989) *J. Biol. Chem. 264*, 7584−7589.
Shin, M. (1973) *Biochim. Biophys. Acta 292*, 13−19.
Shin, M., & Arnon, D. I. (1965) *J. Biol. Chem. 240*, 1405−1411.
Smith, D. B., & Johnson, K. S. (1988) *Gene 67*, 31−40.
Swenson, R. P., & Krey, G. D. (1994) *Biochemistry 33*, 8505−8514.
Towbin, H., Staehelin, T., & Gordon, J. (1979) *Proc. Natl. Acad. Sci. U.S.A. 76*, 4350−4354.
Watt, W., Tulinsky, A., Swenson, R. P., & Watenpaugh, K. D. (1991) *J. Mol. Biol. 218*, 195−208.
Zanetti, G., & Forti, G. (1966) *J. Biol. Chem. 241*, 279−285.
Zanetti, G., Cidaria, D., & Curti, B. (1982) *Eur. J. Biochem. 126*, 453−458.
Zanetti, G., Massey, V., & Curti, B. (1983) *Eur. J. Biochem. 132*, 201−205.

BI950980D